STEM CELLS TRANSLATIONAL MEDICINE®

TISSUE ENGINEERING AND REGENERATIVE MEDICINE

Targeting of ALK2, a Receptor for Bone Morphogenetic Proteins, Using the Cre/lox System to Enhance Osseous Regeneration by Adipose-Derived Stem Cells

JONATHAN R. PETERSON,[a] OLUWATOBI EBODA,[a] SHAILESH AGARWAL,[a] KAVITHA RANGANATHAN,[a] STEVEN R. BUCHMAN,[a] MIN LEE,[b] STEWART C. WANG,[a] YUJI MISHINA,[c] BENJAMIN LEVI[d]

Key Words. Mesenchymal stem cells • ALK2 • Calvarial defect • Bone tissue engineering

[a]Department of Surgery, University of Michigan Medical School, Ann Arbor, Michigan, USA; [b]Division of Advanced Prosthodontics, Biomaterials, and Hospital Dentistry, University of California, Los Angeles, Los Angeles, California, USA; [c]Department of Biologic and Materials Sciences, University of Michigan Dental School, Ann Arbor, Michigan, USA; [d]Department of Surgery, Massachusetts General Hospital, Boston, Massachusetts, USA

Correspondence: Benjamin Levi, M.D., Massachusetts General Hospital, Department of Surgery, 21 Beacon Street, Boston, Massachusetts 02108, USA. Telephone: 847-571-6511; E-Mail: benlevimd@gmail.com

Received April 12, 2014; accepted for publication August 1, 2014; first published online in SCTM *EXPRESS* September 17, 2014.

1066-5099/2014/$20.00/0

http://dx.doi.org/10.5966/sctm.2014-0082

ABSTRACT

Access to readily available autogenous tissue that regenerates bone would greatly improve clinical care. We believe the osteogenic phenotype caused by mutations in ALK2 can be harnessed in adipose-derived stem cells (ASCs) to improve bone tissue engineering. We set out to demonstrate that ALK2 may serve as a novel target to (a) improve in vitro ASC osteogenic differentiation and (b) enhance in vivo bone regeneration and calvarial healing. Transgenic mice were designed using the Cre/lox system to express constitutively active ALK2 (caALK2) with ubiquitously inducible Cre expression after tamoxifen exposure. ASCs from caALK2+/− and caALK2−/− (control) mice were exposed to tamoxifen and assessed for pro-osteogenic gene expression, bone morphogenetic protein (BMP) signaling, and osteogenic differentiation. Next, ASCs collected from these transgenic mice were analyzed in vivo using a calvarial defect model and analyzed by micro-computed tomography (micro-CT) and histology. ASCs from caALK2+/− mice had increased BMP signaling as demonstrated by upregulation of pSmad 1/5. ASCs from caALK2+/− mice had enhanced bone signaling and osteogenic differentiation compared with caALK2−/− mice ($n = 4, p < .05$). Transcription of pro-osteogenic genes at day 7 was significantly higher in ASCs from caALK2-overexpressing mice (*Alp*, *Runx2*, *Ocn*, *Opn*) ($n = 4, p < .05$). Using micro-CT and histomorphometry, we found that bone formation was significantly higher in mice treated with caALK2-expressing ASCs in vivo. Using a novel transgenic mouse model, we show that expression of constitutively active ALK2 receptor results in significantly increased ASC osteogenic differentiation. Furthermore, we demonstrate that this increased ASC differentiation can be harnessed to improve calvarial healing. STEM CELLS TRANSLATIONAL MEDICINE *2014;3:1375–1380*

INTRODUCTION

Bone autograft is currently the gold standard for calvarial reconstruction; however, its use is constrained by availability and donor site morbidity. The use of autogenous adipose-derived stem cells (ASCs) on a matrix scaffold offers a promising alternative to autograft. Recent clinical studies have attempted to augment the osteogenic microenvironment of scaffolds through direct recombinant bone morphogenetic protein-2 (BMP-2) and BMP-7 application [1–3]. Results have been mixed because BMP ligands can have a catabolic effect on bone through expression of RANK ligand-osteoprotegerin pathway. BMP-2 has been shown to induce osteoclastogenesis by upregulation of RANKL, and BMP7 applied to vertebral burst fractures causes bone resorption [4].

Patients with an R206H mutation in ALK2, a type I BMP receptor, develop fibrodysplasia ossificans progressiva (FOP) because of hyperactivation of the ALK2 receptor (caALK2) [5, 6]. This disease is characterized by the formation of heterotopic ossification in the soft tissues [5, 7]. Specifically, BMP-7 has been shown to bind to and form a complex with ALK2 and BMPR2, stimulating phosphorylation of Smad 1/5 by the kinase domain of ALK2. Phosphorylated Smad 1/5 then translocates to the nucleus, upregulating osteogenic gene expression. In this study, we use the Cre/lox system to induce expression of a constitutively activated ALK2 (caALK2) by Q207D mutation in mouse ASCs [8, 9]. We hypothesized that constitutive activity of ALK2 signaling will improve the osteogenic potential of osteopotent cells such as ASCs.

MATERIALS AND METHODS

Animals

The construction of a transgenic mouse line of conditionally expressed, constitutively active ALK2Q207D (CAG-Z-EGFP-caALK2; referred to as

Table 1. Polymerase chain reaction primers

Gene	Forward sequence	Reverse sequence
mRunx2	GTGCGGTGCAAACTTTCTCC	AATGACTCGGTTGGTCTCGG
mOcn	CTGACAAAGCCTTCATGTCCAA	GCGGGCGAGTCTGTTCACTA
mOpn	GCACTCCAACTGCCCAAGA	TTTTGGAGCCCTGCTTTCTG
mAlp	TGAGCGACACGGACAAGA	GGCCTGGTAGTTGTTGTGAG
mGapdh	CAAGGTCATCCATGACAACTTTG	GGCCATCCACAGTCTTCTGG

caALK2 hereafter) has been previously described [8]. Ubiquitin-CreER mice (UBC hereafter), which express a tamoxifen-inducible Cre recombinase ubiquitously under the control of the ubiquitin promoter, were obtained from Jackson Laboratory (Bar Harbor, ME, http://www.jax.org). Cre activity is transient, but Cre expressed (not expressing) cells are positive for green fluorescent protein (GFP), and thus tissue engraftment of Cre recombined (which indicates higher BMP activity) cells can be detected by GFP. Cre unrecombined cell can be detected by nuclear localized β-galactosidase. We have previously shown that implanted ASCs are traceable during the first 2 weeks after implantation [10]. All experiments involving the use of animals were approved by the Institutional Animal Use and Care Committee at the University of Michigan, Ann Arbor (PRO0001553).

Isolation and Osteogenic Differentiation of Primary Adipose-Derived Mesenchymal Cells

ASCs were harvested from the inguinal fat pads of mutant (caALK2+/−; UBC+/−) and littermate control mice (caALK2−/−; UBC+/−, n = 4 per group) as previously described [11]. ASCs were seeded and treated with osteogenic differentiation medium (ODM) supplemented with 4-hydroxy tamoxifen (4OHT, 100 ng/ml; Sigma-Aldrich, St. Louis, MO, http://www.sigmaaldrich.com) [11]. Early osteogenic differentiation was assessed by alkaline phosphatase stain and quantification on day 7 [12]. Alizarin red staining for bone mineral deposition and quantification was completed at day 14 as previously described [13].

Quantitative Polymerase Chain Reaction

RNA was harvested from cells after 7 days in ODM using the RNeasy Mini Kit (Qiagen, Germantown, MD, http://www.qiagen.com), reverse transcription was performed with 1 μg of RNA, and quantitative real-time polymerase chain reaction was carried out as previously described [14, 15]. Specific primers for the genes of interest (*Runx2*, *Osteocalcin* [*Ocn*], *Osteopontin* (*Opn*), *Alkaline phosphatase* [*Alp*]) were chosen based on their PrimerBank sequence (Table 1).

Western Blot Analysis

Cells were lysed and protein was collected after 7 days in osteogenic differentiation medium and assayed with standard immunoblotting technique as previously described [14]. Antibodies against phospho-Smad 1/5 and Smad 5 (Cell Signaling Technology, Beverly, MA, http://www.cellsignal.com) were used. All proteins were normalized with the loading controls (α-tubulin) and quantified by densitometry [14].

Scaffold Creation

Hydroxyapatite-coated poly(lactic-co-glycolic acid) (PLGA) scaffolds were fabricated from 85/15 poly(lactic-coglycolic acid) (inherent viscosity = 0.61 dl/g; Birmingham Polymers, Birmingham, AL, http://www.absorbables.com) by solvent casting and a particulate leaching process as previously described [10].

Calvarial Defects

Nonhealing, critical-sized (4 mm) calvarial defects were created in the right parietal bone of adult CD-1 (60 days old) mice as previously described [10]. Animals were split equally into four treatment groups: (a) empty defects, in which a 4-mm defect was created; (b) scaffold only, in which a scaffold without cells was placed in the defect site; (c) scaffold with 150,000 caALK2+/− ASCs after 4OHT induction; and (d) scaffold with 150,000 4-OHT-treated caALK2−/− ASCs (n = 5 per group). ASCs were not preinduced with ODM prior to implantation.

Micro-CT Analysis

In vivo bone formation was assessed with longitudinal micro-computed tomography (micro-CT) scans for 8 weeks. Images were reconstructed, and bone volume formation was analyzed using a calibrated imaging protocol as previously described. Quantification was performed as previously described, selecting for new, calcified bone with a Hounsfield radio density of 800 or greater [14, 16].

Histologic Processing and Aniline Blue Staining

Eight weeks following defect creation and scaffold placement, whole calvaria were dissected, fixed in neutral buffered formalin overnight, decalcified in 19% EDTA solution, and processed for paraffin embedding. Five-micrometer sections were made in cross-section through the defect and stained for bone tissue with aniline blue.

Statistical Analysis

Means and standard deviations were calculated from numerical data, and statistical analysis was performed using an appropriate analysis of variance. Equivariance was assessed with Levene's test, and a Welch correction was applied when indicated. Post hoc analysis for more than two data sets was completed with Tukey's test with equivariant data or Games-Howell if Levene's test failed. In figures, bar graphs represent means, whereas error bars represent one standard deviation. Significance was defined as $p < .05$.

RESULTS

Verification of caALK-2 Phenotype

Genotyping was performed to verify the presence of the caALK2 ($ALK2^{Q207D}$) gene (Fig. 1A). Concurrently, we observed significantly increased phosphorylation of Smad 1/5 in those ASCs from caALK2+/− mutant mice verifying caALK2 activation (Fig. 1B).

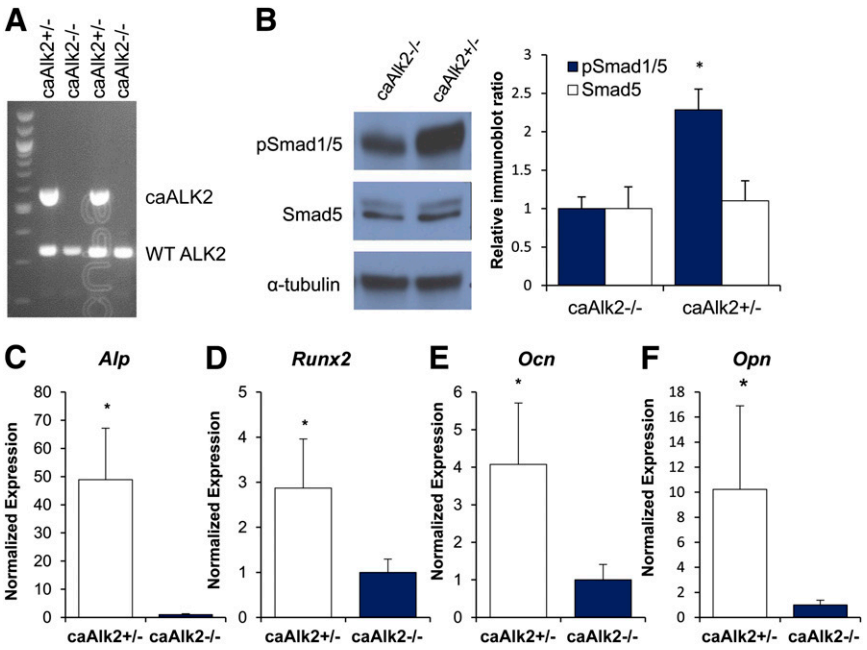

Figure 1. caALK2 confers increased osteogenic signaling among adipose-derived stem cells (ASCs). **(A):** Genotyping results of cells from caALK2+/− and caALK2−/− mice. The wild-type allele shown at the bottom was evident in all samples, whereas the transgene for conditional activation of constitutive caALK2 signaling was present only in caALK2+/− mice. **(B):** Western blot analysis of protein collected from caALK2+/− and caALK2−/− ASCs after 7 days of exposure to osteogenic differentiation medium (ODM) and tamoxifen for phosphorylated (activated) Smad 1/5, Smad 5, and α-tubulin (loading control). Immunoblotting was quantified by densitometry and showed significantly more activation of Smad signaling in the caALK2+/− ASCs. **(C–F):** Quantitative polymerase chain reaction results for osteogenic genes alkaline phosphatase (*Alp*) **(C)**, *Runx-2* **(D)**, osteocalcin (*Ocn*) **(E)**, and osteopontin (*Opn*) **(F)** in caALK2+/− and caALK2−/− ASCs after 7 days of exposure to ODM and tamoxifen. In the charts, the bars represent means, and error bars represent one standard deviation (∗, $p < .05$). Abbreviation: caALK2, constitutively active ALK2.

Mesenchymal Stem Cells Expressing caALK2 Have Increased Osteogenic Signaling In Vitro

Early osteogenic gene markers alkaline phosphatase (*Alp*) and *Runx-2* were 50 and 3 times higher, respectively, in caALK2 mutant ASCs ($n = 4$, $p < .05$) compared with littermate caALK2−/− controls (Fig. 1C, 1D). Similarly, intermediate and late gene markers of osteogenic differentiation *Ocn* and *Opn* were also significantly elevated in caALK2 expressing ASCs ($n = 4$, $p < .05$) (Fig. 1E, 1F).

MSCs That Express caALK2 Have Increased Osteogenic Differentiation In Vitro

We next analyzed the effect of caALK2 expression on early and late osteogenic differentiation of ASCs cultured in vitro. After 7 days in ODM, we noted significantly more alkaline phosphatase staining and quantification of alkaline phosphatase enzyme in ASCs expressing caALK2 (Fig. 2A, 2B). After 14 days of osteogenic differentiation, we noted significantly more bone mineral formed by ASCs expressing caALK2 compared with control (alizarin red stain) (Fig. 2C, 2D).

Scaffolds Seeded With ASCs Expressing caALK2 Enhance Calvarial Healing

ASCs expressing caALK2 were seeded onto hydroxyapatite-coated PLGA scaffolds. Wild-type ASCs without the $ALK2^{Q207D}$ transgene were also seeded at the same density. We observed significantly more bone regeneration in the calvarial defects that had scaffolds seeded with caALK2+/− ASCs than scaffolds with caALK2−/− ASCs, scaffold alone or no scaffold (Fig. 3A, 3B). Confirmation of new bone formation was verified by histologic stain with aniline blue (Fig. 4).

Discussion

Here we demonstrate that caALK2 results in increased osteogenic signaling and osteogenic differentiation of ASCs without supplementation with BMP ligand in vitro and in vivo. Our interest in ALK2 stems from the fact that a known mutation conferring increased ALK2 activity results in FOP [9]. Because no additional signaling molecule or other stimulus is required, the surrounding cells retain their original genotype. The end result of improved bony healing is evident based on the micro-CT scans demonstrating bone formation only within the calvarial defect.

Of note, the calvarial regeneration observed in this study demonstrated less robust in vivo bone growth than suggested by previous studies using human ASCs [14, 17]. This finding may be due to the fact that human ASCs are more osteogenic in vitro and in vivo than mouse ASCs [11]. Additional studies will analyze whether our implanted cells undergo endochondral ossification and whether the early cartilage regenerate is different between mutant and control cells.

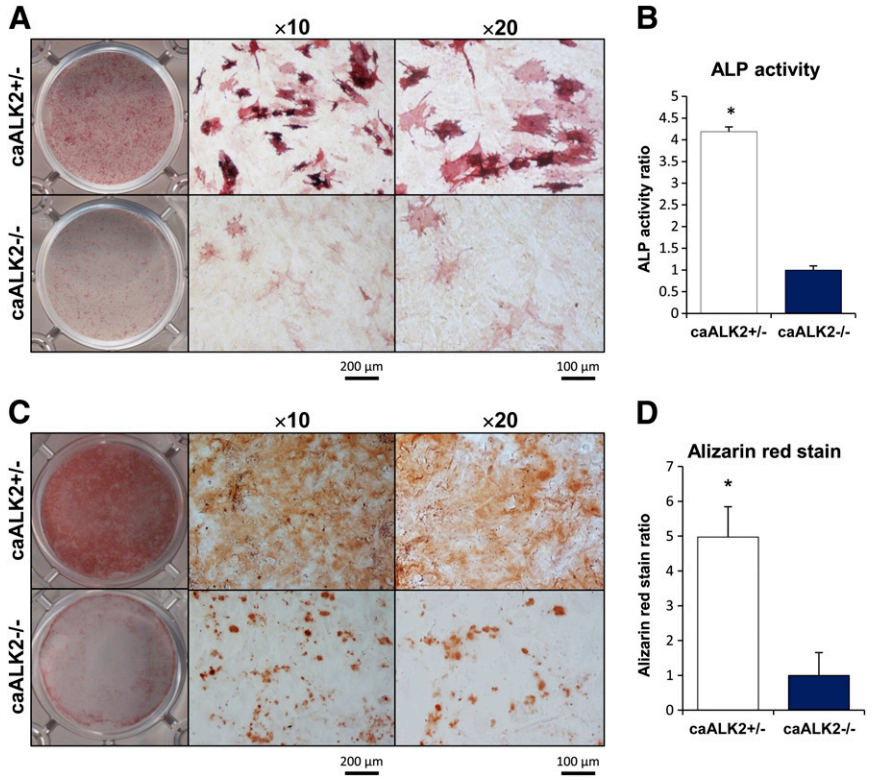

Figure 2. caALK2 activation results in increased in vitro bone formation. **(A):** ALP stain of caALK2+/− and caALK2−/− adipose-derived stem cells exposed to tamoxifen and ODM for 7 days. Positive staining is pink and indicates ALP activity and osteogenic differentiation. Representative microtiter wells are shown at the left with micrograph details shown at ×10 (scale bar = 200 μm) and ×20 magnification (scale bar = 100 μm). **(B):** Quantification of ALP activity normalized to total protein content in these cells. **(C):** Alizarin red stain of these cells after 14 days exposure to osteogenic differentiation medium and tamoxifen. Red staining indicates in vitro osteoid deposition. Representative microtiter wells are shown at the left with micrograph details shown at ×10 (scale bar = 200 μm) and ×20 magnification (scale bar = 100 μm). **(D):** Colorimetric quantification of solubilized alizarin red stain. In the charts, the bars represent means, and error bars represent one standard deviation (*, $p < .05$). Abbreviations: ALP, alkaline phosphatase; caALK2, constitutively active ALK2.

Conclusion

Injuries incurred during trauma and combat often involve extensive traumatic damage to superficial and deep soft tissues of the extremities, axial skeleton, and the craniofacial skeleton, requiring extended hospitalization and prolonged debilitation. These chronic complications can profoundly affect quality of life. Accelerated rehabilitation and reconstruction with this technology, we hope, can reduce hospitalization and forestall serious and chronic complications such as infection, loss of function, and loss of limb. We believe a strategy proven to elicit bony growth from a more osteogenic ASC population is less disruptive to the surrounding environment. The abundance of ASCs in human fat suggests that these cells may be a valuable therapeutic agent if appropriately manipulated. Our model for therapy is not limited to calvarial defects and may apply to long bone fractures, bony gaps following trauma, and spinal fractures, all of which have seen mixed results with addition of exogenous BMP.

Acknowledgments

We thank Amanda Fair and the Center for Molecular Imaging at the University of Michigan for assistance with micro-CT imaging and analysis. B.L. was supported by NIH Grant 1K08GM109105-01 and a Plastic Surgery Foundation National Endowment Award.

Author Contributions

J.R.P. and B.L.: conception and design, collection and/or assembly of data, data analysis and interpretation, manuscript writing, final approval of manuscript; O.E.: collection and/or assembly of data, data analysis and interpretation, final approval of manuscript; S.A.: conception and design, data analysis and interpretation, manuscript writing, final approval of manuscript; K.R.: data analysis and interpretation, manuscript writing, final approval of manuscript; S.R.B. and S.C.W.: conception and design, administrative support, final approval of manuscript; M.L.: provision of study materials, data analysis and interpretation, final approval of manuscript; Y.M.: conception and design, provision of study materials, data analysis and interpretation, final approval of manuscript.

Disclosure of Potential Conflicts of Interest

The authors indicate no potential conflicts of interest.

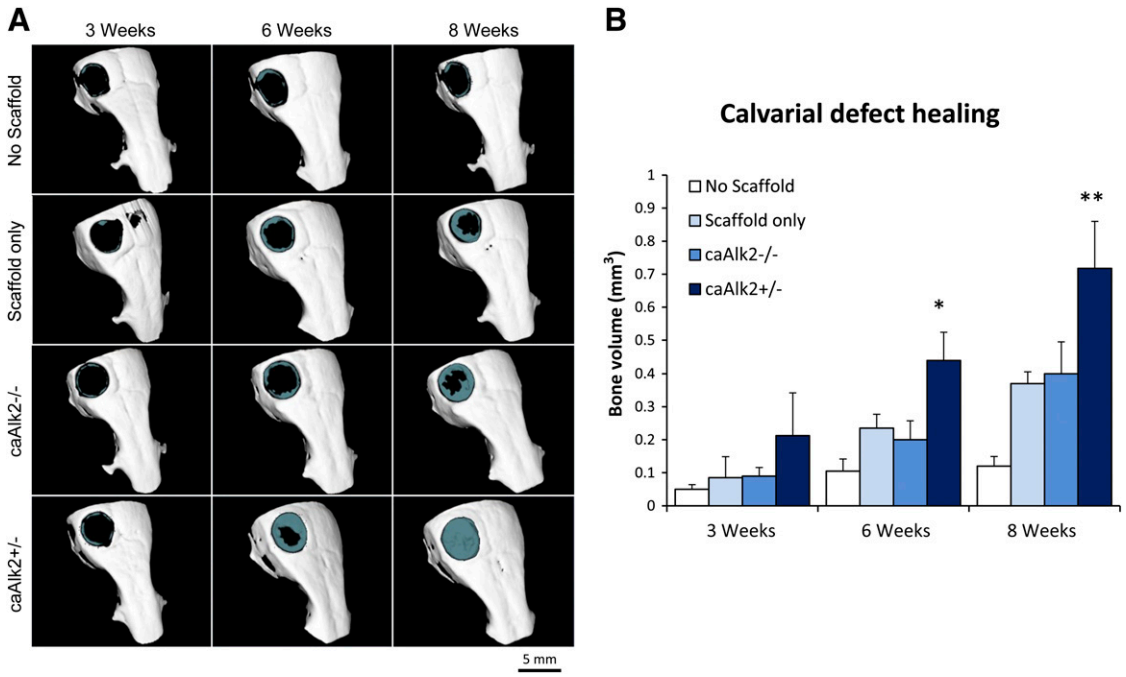

Figure 3. caALK2 expression on implanted scaffolds enhanced calvarial healing. **(A):** Representative micro-computed tomography (micro-CT) reconstructed images of mouse calvarial defects with the following treatments: no scaffold, scaffold alone, scaffold with caALK2−/− adipose-derived stem cells (ASCs), or scaffold with caALK2+/− ASCs. Cells were treated with tamoxifen prior to implantation into the scaffolds. Micro-CT scans were completed at 3, 6, and 8 weeks following defect creation. In the images, purple coloration indicates healing of the defect (scale bar = 5 mm). **(B):** Quantification of new-growth bone volume in the defects at the various scan time points (*, $p < .05$; **, $p < .01$). Abbreviation: caALK2, constitutively active ALK2.

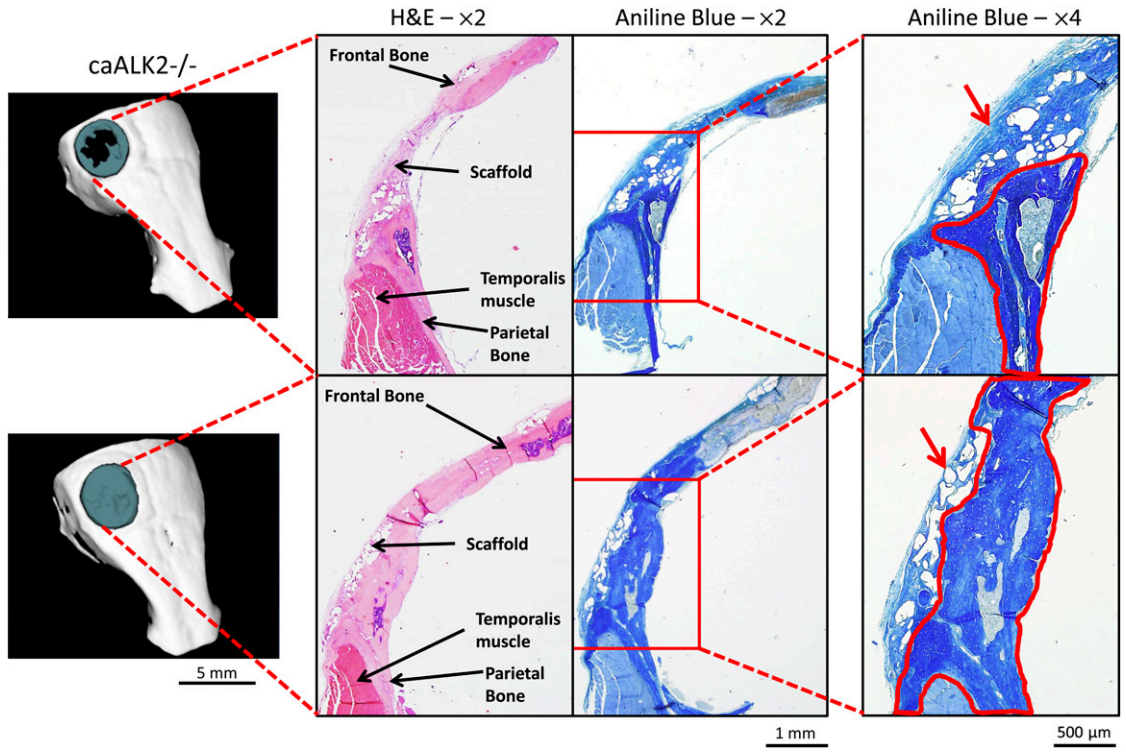

Figure 4. Histologic analysis of calvarial defect treated with a scaffold with caALK2−/− or caALK2+/− adipose-derived stem cells (ASCs). Representative micro-computed tomography reconstructed images of mouse calvarial defects receiving scaffold with caALK2−/− or caALK2+/− ASCs are shown at the left (scale bar = 5 mm). Cross-sections through the defect were made, and representative slides that showed the most bone growth were stained with H&E or aniline blue. H&E panels at ×2 magnification (scale bar = 1 mm) are labeled with anatomic landmarks. Aniline blue panels at ×2 magnification (scale bar = 1 mm) and ×4 magnification (scale bar = 500 μm) exhibit bone staining in dark blue. New bone growth is outlined in red in the detail panels, and red arrows indicate scaffold absent of new bone. Abbreviations: caALK2, constitutively active ALK2; H&E, hematoxylin and eosin.

References

1 Lewandrowski KU, Nanson C, Calderon R. Vertebral osteolysis after posterior interbody lumbar fusion with recombinant human bone morphogenetic protein 2: A report of five cases. Spine J 2007;7:609–614.

2 Perri B, Cooper M, Lauryssen C et al. Adverse swelling associated with use of rh-BMP-2 in anterior cervical discectomy and fusion: A case study. Spine J 2007;7:235–239.

3 Robin BN, Chaput CD, Zeitouni S et al. Cytokine-mediated inflammatory reaction following posterior cervical decompression and fusion associated with recombinant human bone morphogenetic protein-2: A case study. Spine 2010;35:E1350–E1354.

4 Laursen M, Høy K, Hansen ES et al. Recombinant bone morphogenetic protein-7 as an intracorporal bone growth stimulator in unstable thoracolumbar burst fractures in humans: Preliminary results. Eur Spine J 1999;8:485–490.

5 Shore EM, Xu M, Feldman GJ et al. A recurrent mutation in the BMP type I receptor ACVR1 causes inherited and sporadic fibrodysplasia ossificans progressiva [published correction appears in Nat Genet 2007;39:276]. Nat Genet 2006;38:525–527.

6 Smith GL, Smith BD, Giordano SH et al. Risk of hypothyroidism in older breast cancer patients treated with radiation. Cancer 2008; 112:1371–1379.

7 Medici D, Shore EM, Lounev VY et al. Conversion of vascular endothelial cells into multipotent stem-like cells. Nat Med 2010;16: 1400–1406.

8 Fukuda T, Scott G, Komatsu Y et al. Generation of a mouse with conditionally activated signaling through the BMP receptor, ALK2. Genesis 2006;44:159–167.

9 Yu PB, Deng DY, Lai CS et al. BMP type I receptor inhibition reduces heterotopic [corrected] ossification. Nat Med 2008;14:1363–1369.

10 Levi B, James AW, Nelson ER et al. Human adipose derived stromal cells heal critical size mouse calvarial defects. PLoS One 2010;5:e11177.

11 Levi B, Nelson ER, Brown K et al. Differences in osteogenic differentiation of adipose-derived stromal cells from murine, canine, and human sources in vitro and in vivo. Plast Reconstr Surg 2011;128:373–386.

12 James AW, Xu Y, Wang R et al. Proliferation, osteogenic differentiation, and fgf-2 modulation of posterofrontal/sagittal suture-derived mesenchymal cells in vitro. Plast Reconstr Surg 2008;122:53–63.

13 Xu Y, James AW, Longaker MT. Transforming growth factor-beta1 stimulates chondrogenic differentiation of posterofrontal suture-derived mesenchymal cells in vitro. Plast Reconstr Surg 2008;122:1649–1659.

14 Levi B, Hyun JS, Nelson ER et al. Nonintegrating knockdown and customized scaffold design enhances human adipose-derived stem cells in skeletal repair. Stem Cells 2011;29:2018–2029.

15 Levi B, Nelson ER, Li S et al. Dura mater stimulates human adipose-derived stromal cells to undergo bone formation in mouse calvarial defects. Stem Cells 2011;29:1241–1255.

16 Brown SA, Levi B, Lequeux C et al. Basic science review on adipose tissue for clinicians. Plast Reconstr Surg 2010;126:1936–1946.

17 Culbert AL, Chakkalakal SA, Theosmy EG et al. Alk2 regulates early chondrogenic fate in fibrodysplasia ossificans progressiva heterotopic endochondral ossification. Stem Cells 2014; 32:1289–1300.